TÜBİTAK

Turkish Journal of Chemistry

http://journals.tubitak.gov.tr/chem/

Research Article

Turk J Chem
(2021) 45: 1004-1015

doi:10.3906/kim-2012-47

Novel mixed ligand coordination compounds of some rare earth metal cations containing acesulfamato/*N,N*-diethylnicotinamide

Leriman ZEYBEL, Dursun Ali KÖSE*
Department of Chemistry, Science and Arts Faculty, Hitit University, Çorum, Turkey

Received: 20.12.2020 • **Accepted/Published Online:** 26.04.2021 • **Final Version:** 27.08.2021

Abstract: The mixed ligand coordination compounds containing acesulfamato and *N,N*-diethylnicotinamide biomolecules of some rare earth metal cations (Eu^{3+}, Tb^{3+}, Ho^{3+}, Er^{3+} and Yb^{3+}) were synthesized, and their structural properties were investigated. Possible structural formulas have been proposed by determining the chemical composition of molecules (elemental analysis), binding properties (infrared spectroscopy, mass analysis, solid-state UV-vis spectroscopy), thermal degradation properties (TGA / DTA curves). Based on the data collected, it is suggested that rare earth metal cations with a 3+ oxidation state have sextet coordination. The geometries of the structures were thought to be distorted octahedral. The charge balance of the coordination sphere is balanced by a monoanionic acesulfamato located outside the coordination sphere. When the thermal behaviours of the complexes were examined, it was determined that the compounds with Eu^{3+}, Tb^{3+}, and Yb^{3+} metal cations contained one hydrate water outside the coordination sphere. Hydrate waters do not exist in the Ho^{3+} and Er^{3+} metal cation-centred complexes. At the end of the thermal decomposition analysis of all complex structures, it was determined that they leave the relevant metal oxides in the reaction vessels as final decomposition products.

Key words: Rare-earth metal complexes, acesulfamato, *N,N*-diethylnicotinamide, structural characterization, thermal analysis, mixed ligand complexes

1. Introduction

Studies on the coordination compounds of rare earth metal (REM) cations started later than studies on transition metals. The complex compounds formed by rare earth metal cations with organic ligands have rich chemistry, unique physical properties, different and essential application areas. For this reason, interest in these compounds has been increasing for the last half-century. Due to their characteristic photophysical and magnetic properties, their use in magnetic and optical devices [1–6], sensor systems [7], biological analysis applications [8–10], and medical diagnostic devices [11–14] is increasing.

Rare earth metal cations prefer to form metal complexes with high coordination numbers with hard Lewis-based donors such as F, O, and N due to their strong Lewis acid character and large ionic radii. The carboxylic acids containing strong Lewis donor atoms, such as O and N, and polyaminopolycarboxylic acids are among the most suitable coordination ligands for rare earth metal cations with 3+ oxidation steps and meet the high coordination numbers needed [15,16].

Today, in biological applications, clinical studies, NLO (nonlinear optics) applications, OLED (organic light-emitting diode) applications, MOF (metal-organic framework) compounds [17–19] and even corrosion inhibitors with traditional and toxic chromate-based compounds demonstrated potential for use [20]. On the other hand, the increasing use of rare earth metal compounds in clinical treatments and medicines may raise some negative concerns about their long- and short-term effects in humans and animals. One of the most important physiological effects of rare earth metal cations is their ability to block both voltage-operated and receptor-operated calcium channels [21–23]. Approximately 100 complex structures containing the aminoacid ligament, which is considered an important ligand group for rare earth metal cations, were examined and characterized by X-ray single-crystal analysis [23,24]. Large rare earth metal cations, depending on their radius, generally prefer to form coordination compounds with high coordination numbers (7–10). However, coordination compounds forming six coordinated complex structures with ligands showing strong electron donor properties are rarely reported in the literature [25–29].

Acesulfamato ($C_4H_4SO_4NH$, HAcs, Figure 1) is an oxathiazinone dioxide discovered by Clauss [30] in 1967 and has been widely used as an artificial sweetener since 1988 [31] after the FDA (Food and Drug Administration) [32].

* Correspondence: dalikose@hitit.edu.tr

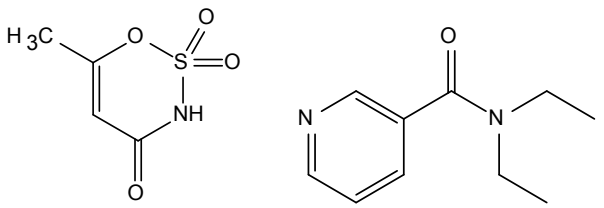

(a) (b)

Figure 1. Molecular formula of acesulfamato (a) and *N,N*-diethylnicotinamide (b).

Acesulfame anion ($C_4H_4SO_4N^-$, *acs*$^-$) is an interesting and versatile ion. It is an exciting molecule with donor acidic imino nitrogen, one carbonyl and two sulfonyl oxygen. These donor atoms can exhibit structural diversity by differently coordinating their metal centres. Acesulfame anion, nicotinamide [33,34], N,N-diethylnicotinamide (Fig. 1b) [35], 3-aminopyridine [36], N,N-dimethylethylenediamine [37], 2-aminopyrimidine [38], etc. tend to form crosslinked metal complexes with neutral ligands that have strong electron donating groups. It can also serve as the stabilizing anion of the coordination compounds formed by this type of ligands. In acesulfame metal complexes, via the acidic imino nitrogen atom coordinated to the metal cation [$(Co(acs)_2(H_2O)_4]$ [39], via the carbonyl oxygen atom [$Ni(acs)_2(H_2O)_4$] [40] or as in the complex structure of [$Cu(ampy)_2(acs)_2$] [35,38], compounds with which a coordination is made through both donor atoms were synthesized.

In this study, coordination compounds with mixed ligands of acesulfame (*acs*) and *N,N*-diethylnicotinamide (nikethamide, *dena*) of the rare earth metal cations Eu^{3+}, Tb^{3+}, Ho^{3+}, Er^{3+}, and Yb^{3+} were synthesized. Afterwards, the structural characterizations of the molecules were examined, and their thermal degradation steps were investigated in detail.

2. Materials and methods

The chemicals used in synthesis reactions [$Eu(ClO_4)_3.6H_2O$ (europium(III)perchlorate hexahydrate, 50% w/w in aq. soln.), $Tb(ClO_4)_3$ (terbium(III)perchlorate, 50% w/w in aq. soln.), $Ho(ClO_4)_3$ (holmium(III)perchlorate, 50% w/w aq. soln.), $Er(ClO_4)_3.6H_2O$ (erbium(III)perchlorate, 50% w/w in aq. soln.), $Yb(ClO_4)_3$ (ytterbium(III)perchlorate, 50% w/w in aq. soln.), potassium acesulfame and *N,N*-diethylnicotinamide] were obtained from Alfa-Easer reagent grade.

2.1. Synthesis of complexes

In the synthesis of the complexes, perchlorate salts of 0.01 mol Eu^{3+}, Tb^{3+}, Ho^{3+}, Er^{3+} and Yb^{3+} cations were dissolved in 30 mL of water, 20 mL of the aqueous solution of 0.03 mol of acesulfame-K was added to the solution obtained. The potassium perchlorate ($KClO_4$) was expected to settle from the continuously stirred solution. Some cold ethyl alcohol was added to the solution to make the precipitation process better. After precipitation, filtration was carried out, and 50 mL of an aqueous solution of 0.02 mol of nicotinamide was added to the solution. The total solution mixed over a magnetic stirrer for 2 h was stored at room conditions for crystallization. The visualization of two-stage general synthesis reactions of mixed ligand metal-acesulfame/*N,N*-diethylnicotinamide complexes is given in Figure 2. Elemental analysis results of metal-acesulfame/*N,N*-diethylnicotinamide complexes are given in Table 1.

2.2. Infrared (FT-IR) spectroscopy

FT-IR spectra of acesulfamato-diethylnicotinamide complexes of synthesized rare earth metal cations (Eu^{3+}, Tb^{3+}, Ho^{3+}, Er^{3+} and Yb^{3}) were recorded in the 4000–400 cm^{-}1 range (Figure 3), and characteristic vibration bands were determined, and the relationships between the structures of the complexes and these vibrations were investigated. In order to learn more about the coordination properties of the complexes, the stretching vibrations of the acesulfamate ligand groups such as imine, carbonyl and sulfonyl were compared to the vibrations of the potassium acesulfamato salt, and the changes in the vibrations were examined. The violent and broad peaks seen in the infrared spectra of the complexes in the range of 3650 cm^{-1}–2850 cm^{-1} can belong to the aqua –O-H group stress vibrations. Aromatic -C-H stretching vibrations in the structure of the ligands appeared as sharp and severe peaks in the range of 2987 cm^{-1}–2979 cm^{-1}. There was no shift towards the low region, indicating coordination in stress vibrations attributable to two different carbonyl groups in the structure of the ligands. This situation indicates that (-C=O) groups do not participate in coordination. In the complexes, the peaks, which are thought to belong to the carbonyl group of the acesulfamato ligand, were observed at very close values between 1660 cm^{-1}–1650 cm^{-1}. The carbonyl ligand of the amide group in the nikethamide ligand appeared in the range of 1615

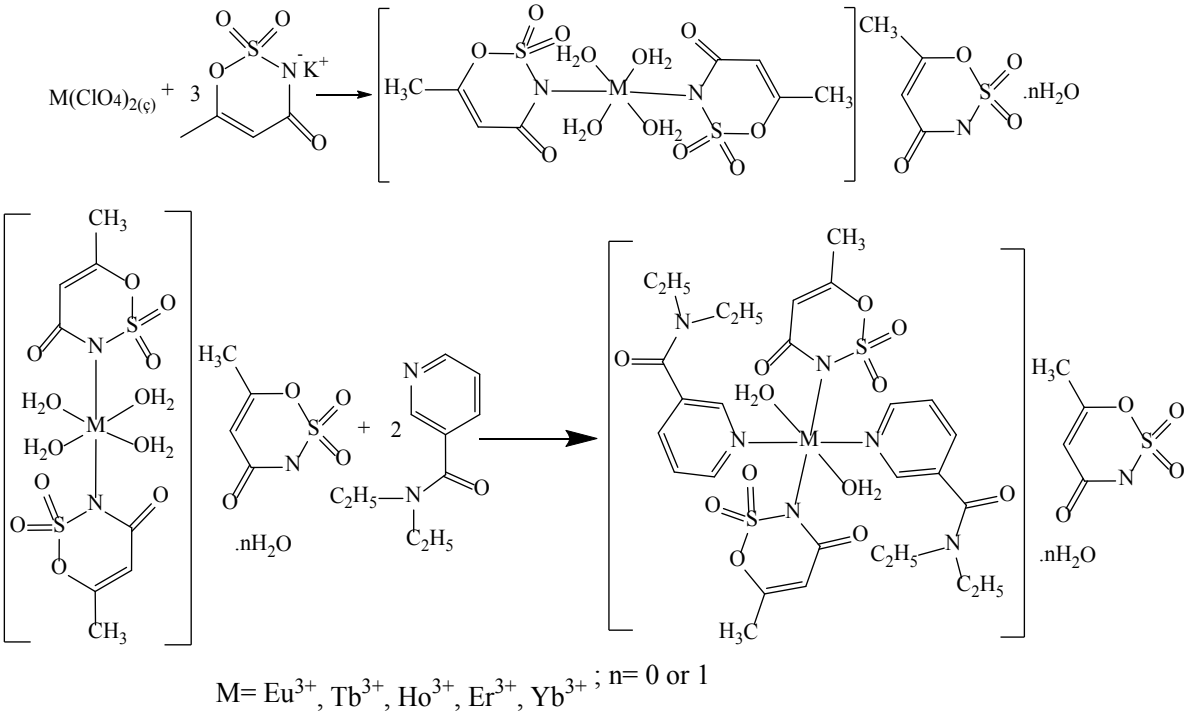

Figure 2. The synthesis reaction of mixed ligand complexes of rare-earth metal-acesulfame/*N,N*-diethylnicotinamide.

Table 1. Elemental analysis data of mixed ligand complexes of rare-earth metal-acesulfamato/*N,N*-diethylnicotinamide.

Complexes	M.W. (g/mol)	Yield (%)	Chemical Analysis (%) Exp. (Theo.)				Colour	Decomp. Temp.(°C)
			C	H	N	S		
$[Eu(acs)_2(dena)_2(H_2O)_2](acs).H_2O$ $C_{32}H_{46}EuN_7O_{17}S_3$	1048.90	57	37.03 (36.64)	4.98 (4.42)	9.51 (9.35)	9.66 (9.17)	pale pink	100
$[Tb(acs)_2(dena)_2(H_2O)_2](acs).H_2O$ $C_{32}H_{46}N_7O_{17}S_3Tb$	1055.86	55	36.82 (36.40)	5.13 (4.39)	9.40 (9.29)	9.43 (9.11)	pale pink	93
$[Ho(acs)_2(dena)_2(H_2O)_2](acs)$ $C_{32}H_{44}HoN_7O_{16}S_3$	1043.85	63	36.25 (36.82)	5.16 (4.25)	9.32 (9.39)	8.87 (9.22)	pale pink	86
$[Er(acs)_2(dena)_2(H_2O)_2](acs)$ $C_{32}H_{44}ErN_7O_{16}S_3$	1046.18	60	36.36 (36.74)	4.93 (4.24)	9.43 (9.37)	9.71 (9.19)	white	104
$Yb(acs)_2(dena)_2(H_2O)_2](acs).H_2O$ $C_{32}H_{46}N_7O_{17}S_3Yb$	1069.99	50	36.21 (35.92)	5.08 (4.33)	9.29 (9.16)	8.31 (8.99)	pale pink	91

cm^{-1}–1605 cm^{-1}. It was determined that the tensile vibrations of the C-N-C groups in the structure of both ligands, which do not coordinate, shift to lower regions than the peaks that can be attributed to these groups. This can be given as evidence that coordination in both ligands takes place over the -N atom in these groups. These coordination connections are also compatible with the literatüre [33–39]. While the stretching vibrations of the acesulfamato ligand belonging to the C-N-C group were observed in the range of 1363 cm^{-1}–1356 cm^{-1}, the stretching vibrations of the C-N-C group in the pyridine ring of the nicotinamide ligand occurred in the ranges of 1395 cm^{-1}–1393 cm^{-1}. The difference between the asymmetric and symmetrical stress vibrations of the SO_2 group can be demonstrated as evidence that the acesulfamato group does not coordinate. The difference between $n(SO_2)_{asym}$ and $n(SO_2)_{sym}$ strain vibrations remains below 140 cm^{-1} in cases where

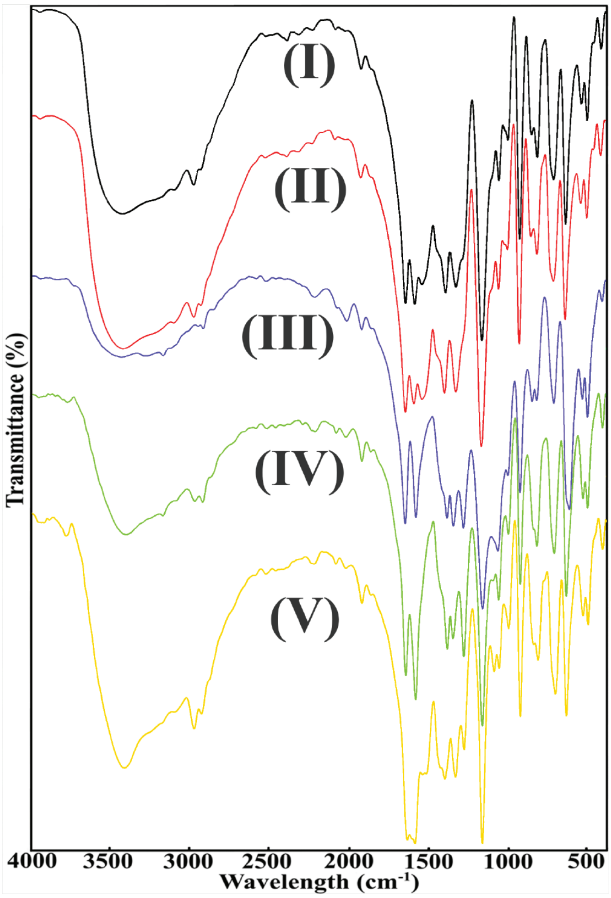

Figure 3. FT-IR spectra of mixed ligand complexes of rare-earth metal-acesulfamato/*N,N*-diethylnicotinamide.

coordination is not achieved over the SO_2 group [41–43]. In the complexes of rare earth elements synthesized, this value is in the range of 112 cm^{-1}–119 cm^{-1}. The peaks that can be attributed to the coordination of the ligands to metal cations are identified. Accordingly, while the coordination of acesulfamato takes place through the anionic -N group, $n(M\text{-}N)_{acs}$ stress vibrations occur in the given order of metal cations in the regions of 629 cm^{-1}, 653 cm^{-1}, 649 cm^{-1}, 649 cm^{-1} and 620 cm^{-1}, respectively. The vibrations related to the coordination of the $n(M\text{-}N)_{pyrd}$ group over the pyridine nitrogen of the nicotinamide ligand were detected in the regions of 675 cm^{-1}, 668 cm^{-1}, 673 cm^{-1}, 673 cm^{-1} and 645 cm^{-1}, respectively. The vibration peaks of aqua binding, which can be attributed to the coordination of aqua ligands in the complex structures (M-O), occurred in the regions of 512 cm^{-1}, 518 cm^{-1}, 516 cm^{-1}, 516 cm^{-1} and 516 cm^{-1}, respectively. The peaks that can be attributed to the significant binding vibrations of complex structures are summarized in Table 2.

2.3. Thermal analysis

Thermal analysis studies of the complex compounds (TG-DTG, DTA) were performed with the Shimadzu DTG-60H system in an inert nitrogen atmosphere (100 mL/min), at a heating rate of 10 °C / min, using a platinum pan using α-Al_2O_3 as a reference. The weight reduction caused by volatile products withdrawing from the structures as a result of the decomposition of the compounds was calculated from the TG curves. The reduced weight ratios and metal-ligand ratios from the last remaining degradation products were found.

When the DTG curve of the Eu(III) mixed ligand (**I**) complex is examined, it is seen that it degrades in six steps. In the first decomposition step, hydrate water is removed (exp:2.07%; calc:1.72%). In the next dehydration step, two aqua ligands coordinated with the metal are decomposed and removed from the structure (exp:3.34%; calc:3.43%).

The degradation of organic ligands begins by forming $3/2SO_2$ gas of the sulfo group (both coordinated and acting as a counter-ion) from acesulfameto (*acs*) molecules (exp:9.02%; calc:9.16%). The fourth degradation step is the step in which organic residues continue to decompose, and the neutral ligand *N,N*-diethylnicotinamide (*dena*) begins to decompose together with the acesulfamato ligand (Table 3).

Table 2. Significant FT-IR peaks of mixed ligand complexes of rare-earth metal-acesulfamato/*N,N*-diethylnicotinamide.

Gruplar	Eu-*acs-dena*	Tb-*acs-dena*	Ho-*acs-dena*	Er-*acs-dena*	Yb-*acs-dena*
$n(OH)_{H2O}$	3560–2850	3560–3380	3650–2850	3650–3150	3550–3150
n(–C–H)	2985	2987	2979	2981	2983
n(C=C)	2222	2221	2227	2228	2229
$n(C=O)_{acs}$	1660	1650	1655	1654	1652
$n(C=O)_{dena}$	1615	1613	1610	1605	1607
n(C=C)	1467	1499	1540	1540	1554
$n(C–N–C)_{acs}$	1357	1356	1357	1357	1363
$n(C–N–C)_{dena}$	1395	1396	1393	1393	1394
$n_{as}(SO_2)/n_s(SO_2)$	1289/1177	1286/1172	1314/1199	1314/1195	1319/1203
$n_{as\text{-}s}$	112	114	115	119	116
n(ring)	1098–827	1078–831	1061–834	1060–833	1090–840
$n_s(CNS)/n_{as}(CNS)_{acs}$	1322/939	1331/943	1323/935	1321/934	1309/938
n(C–N)	1007–727	1015–732	1013–735	1014–734	1014–723
$n(M–N)_{acs}$	629	653	649	649	620
$n(M–N)_{dena}$	675	668	673	673	645
$n(M–O)_{aqua}$	512	518	516	516	516

The next step in the temperature range of 350–450 °C is the step where the last residue of the dena ligand (two C_5H_4N) burns away from the structure (exp:14.16%; calc:14.89%).

In the last decomposition phase, it was predicted that the C_2HNO_2S in the sphere in the coordination area and the other C_2HNO_2 ligand in the counter-ion position were degraded and 1/2 $Eu_2(SO_4)_3$ remained as the final product (exp:29.77%; calc:28.23%).

When the degradation curve and decay steps of the Tb(III) metal cation-centered complex were examined, it was found that it showed similarities with the Eu(III) metal cation complex. Unlike the Eu(III) complex, it is suggested that in this structure, SO_2 gas exit does not occur in a separate step, but in the degradation step of the *dena* ligand. It is believed that the sulfate salt [1/2 $Tb_2(SO_4)_3$; exp:29.43%; calc:28.71%)] remains in the reaction vessel as the final decomposition product in this complex. Details of the degradation steps of the complex are summarized in Table 3.

The thermal analysis data of the metal cation-centered complex structures of Ho(III) (**III**), Er(III) (**IV**), and Yb(III) (**V**) are quite similar. It is predicted that in the thermal decomposition that occurs in five stages in the Ho(III) and Er(III) complexes, which are thought to not contain hydrate waters, two aqua ligands, which are coordinated in the structures, are firstly removed (exp: 3.42%; calc: 3.45% for Ho(III) and exp: 4.04%; calc: 3.44% for Er(III)). In the second step, it is thought that the *acs* ligand for both complexes begins to decay, giving 2 SO_2 gas for Ho(III) and 3 SO_2 gas for Er(III).

It is thought that two groups of $C_5H_{10}NO$ related to the degradation of the *dena* ligand in the next step were removed. In the third decay step of the Ho(III) complex, the remaining SO_2 group of the *acs* ligand, three CH_3 residues and the remaining organic residues of the *dena* ligands are removed. In the specified degradation step of the Er(III) complex, organic residues of *dena* ligands move away from the structure (Table 3). It is believed that in the last decay steps of both complexes, the remaining organic residues are burned off and the oxide compounds of the corresponding metal cations remain as the final decomposition product [exp: 17.07%; calc: 18.10% for Ho(III) and exp: 17.12%; calc: 18.28% for Er(III)].

When the DTG curve of the Yb(III) mixed ligand (**V**) complex is examined, it is seen that it degrades in four stages. In the first decay phase, it is predicted that a total of three aqua molecules in the structure, one hydrate water and two coordination water, are removed. The next degradation step is the degradation step that can be attributed to the degradation of the sulfonyl groups (3 SO_2) and organic residues (3 C_3H_4) of the *acs* ligands (exp:29.51%; calc: 29.19%). It is suggested that in the third decay step, two $C_5H_{10}NO$ organic residues of *dena* ligands are cleaved (exp: 19.11%; calc: 18.72%). In the last decomposition step, it is claimed that all organic residues in the structure burned away and 1/2 Yb_2O_3 oxide compound remained (exp: 17.63%; calc: 18.42%). The compatibility of experimental and calculated weight losses also supports this situation.

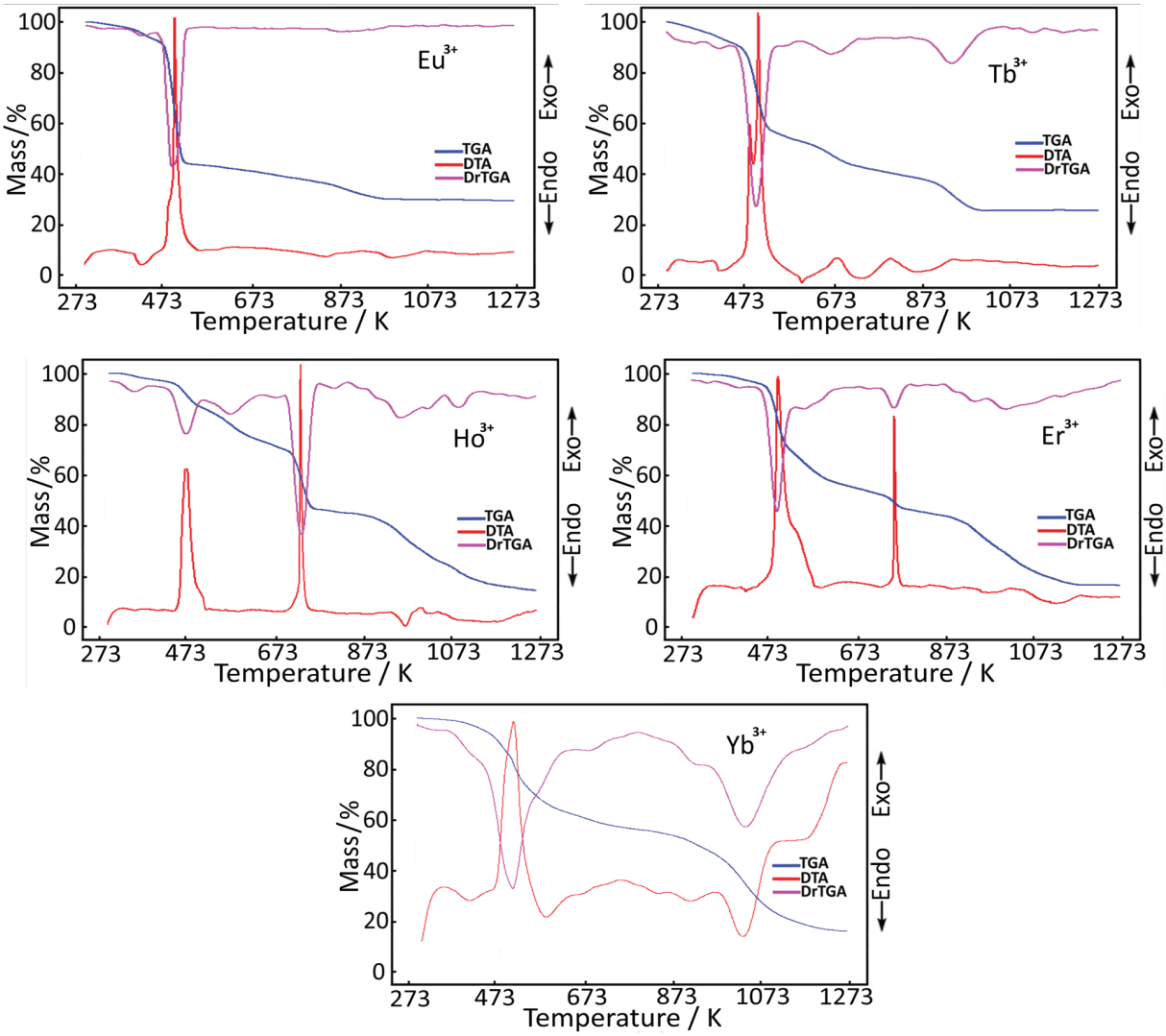

Figure 4. Thermal analysis curves of mixed ligand complexes of rare-earth metal-acesulfamato/*N,N*-diethylnicotinamide.

The thermal analysis curves of the lanthanide group metal cation complexes are given in Figure 4. Data showing the degradation steps and details are summarized in Table 3. The presence of related metal oxide and sulfate compounds, which are the products of the final degradation step resulting from thermal analysis of metal cation complex compounds, was confirmed by powder x-ray analysis.

2.4. Solid-state UV-vis-NIR spectroscopy

When the recorded solid-state UV-VIS-MR spectroscopy curves of lanthanide semi-group metal ions with a charge value of 3+ are examined, a distinct peak in the 850–400 nm range corresponding to the band transition regions of the metals was not observed (Figure 5). The transition of the electrons to high energy levels in the final orbital *"f"* orbitals of the cationic rare earth elements that undergo splitting under UV light was not observed. All complexes are either colourless or almost pale pink in colour. There are breaks that can be interpreted as small vibration peaks in all the synthesized complex structures of only Ho^{3+} metal cation. This situation can be attributed to the increasing electron density in the Ho^{3+} cation compared to the Eu^{3+} and Tb^{3+} cations. The reason why it is not observed in Er^{3+} and Yb^{3+} metal cation complexes can be explained by the restriction of metal cations due to lanthanide shrinkage. For this reason, the Ho^{3+} metal cation centred complexes have a more off-white or pale pink colour than others.

Since lanthanide ions with 3+ oxidation state will not be oxidized, these transitions may be caused by ligands. Therefore, the high-intensity transition peaks (M-L) occurring in the 400–200 nm region of all metal complexes can be attributed to electron transitions from metal to ligands.

Table 3. Thermal analysis data of mixed ligand complexes of rare-earth metal-acesulfamato/*N,N*-diethylnicotinamide.

Complex		Temperature Range (°C)	DTA_{max} (°C)	Leaving Group	Mass Loss (%)		Remained Product (%)		Decomp. Product	Colour
					Exp.	Theor.	Exp.	Theor.		
$[Eu(C_4H_4NO_4S)_2(C_{10}H_{14}N_2O)_2(H_2O)_2](C_4H_4NO_4S).H_2O$ $C_{32}H_{46}EuN_7O_{17}S_3$ **1048.90 g/mol**	1	42–99	89	H_2O	2.07	1.72				pale-pink
	2	100–185	144	$2H_2O$	3.34	3.43				
	3	186–220	–214	$3/2SO_2$	9.02	9.16				
	4	269–427	335	$2C_5H_{10}NO;3C_2H_3$	26.52	26.83				
	5	428–718	450;586	$2C_5H_4N$	14.16	14.89				
	6	719–931	737	$3C_2HNO$	15.12	15.74	29.77	28.23	$1/2Eu_2(SO_4)_3$	black
$[Tb(C_4H_4NO_4S)_2(C_{10}H_{14}N_2O)_2(H_2O)_2](C_4H_4NO_4S).H_2O$ $C_{32}H_{46}N_7O_{17}S_3Tb$ **1055.86 g/mol**	1	42–92	80	H_2O	1.62	1.71				white
	2	93–170	140	$2H_2O$	3.17	3.41				
	3	171–263	–223; –251	$2C_5H_{10}NO;3/2SO_2$	27.67	28.07				
	4	264–451	338	$2C_5H_4N;3C_2H_3$	22.91	22.48				
	5	452–740	477;603	$3C_2HNO$	15.20	15.63	29.43	28.71	$1/2Tb_2(SO_4)_3$	black
$[Ho(C_4H_4NO_4S)_2(C_{10}H_{14}N_2O)_2(H_2O)_2](C_4H_4NO_4S)$ $C_{32}H_{44}HoN_7O_{16}S_3$ **1043.85 g/mol**	1	77–165	87	$2H_2O$	3.42	3.45				pale-pink
	2	166–250	–206	$2SO_2$	12.22	12.27				
	3	251–437	305	$2C_5H_{10}NO$	18.67	19.18				
	4	438–502	–464	SO_2; $3CH_3$; $2C_5H_4N$	25.35	25.41				
	5	503–791	703;772	$3C_3HO$; $3/2N_2O$	20.88	21.57	17.07	18.10	$1/2Ho_2O_3$	black
$[Er(C_4H_4NO_4S)_2(C_{10}H_{14}N_2O)_2(H_2O)_2](C_4H_4NO_4S)$ $C_{32}H_{44}ErN_7O_{16}S_3$ **1046.18 g/mol**	1	104–186	146	$2H_2O$	4.04	3.44				pale-pink
	2	185–266	–243	$3SO_2$	19.13	18.37				
	3	267–476	314	$2C_5H_{10}NO$	19.57	19.13				
	4	477–533	–521	$2C_5H_4N$	13.86	14.93				
	5	558–877	670;785	$3C_4H_4O$; $3/2N_2O$	24.82	25.83	17.12	18.28	$1/2Er_2O_3$	black
$Yb(C_4H_4NO_4S)_2(C_{10}H_{14}N_2O)_2(H_2O)_2](C_4H_4NO_4S).H_2O$ $C_{32}H_{46}N_7O_{17}S_3Yb$ **1069.99 g/mol**	1	78–179	146	H_2O; $2H_2O$	5.42	5.05				white
	2	180–285	–243	$3SO_2$; $3C_3H_4$	29.51	29.19				
	3	286–606	404;573	$2C_5H_{10}NO$	19.11	18.72				
	4	607–820	646;764	$2C_5H_4N$; $3CO$; $3/2N_2O$	27.97	28.62	17.63	18.42	$1/2Yb_2O_3$	black

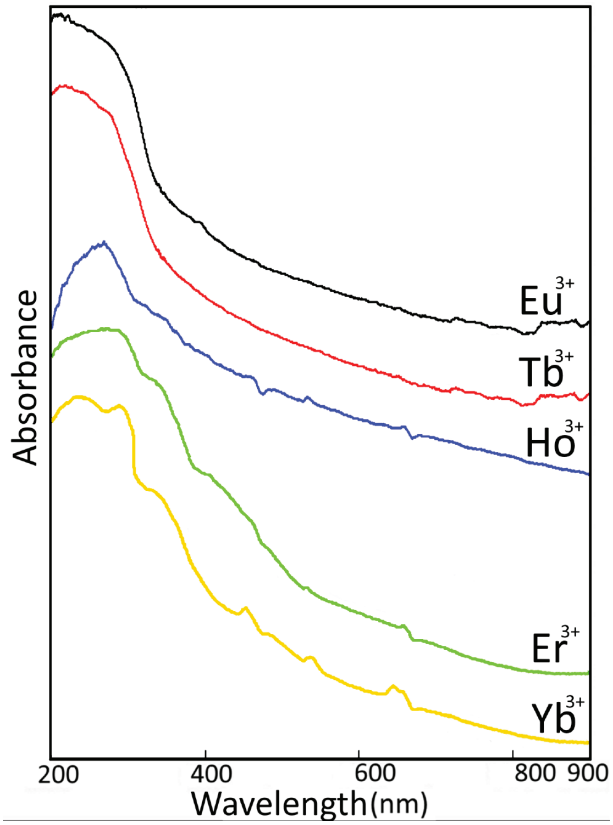

Figure 5. Solid-state UV-vis spectra of rare-earth metal-acesulfamato/*N,N*-diethylnicotinamide mixed ligand complexes.

2.5. Mass spectroscopy

The GC-MS pattern of Eu^{3+} complex and possible cleavage products in the 0–1000 m/z region are given in Figure 6. The mass spectrum patterns of the other four complexes are shown in Figure SF1 in the supplementary file. Similarities were also observed in the recorded GC-MS cleavage products of the coordination compounds thought to have similar structural formulas. Due to the molecular weights of the structures greater than 1000 m/z, the peak values attributable to the molecular ion peaks of the compounds could not be observed. Molecular ion peaks of the dehydrated structure formed due to the removal of the ligand water from the structures were determined. Afterwards, molecular ion peaks were recorded that could be attributed to the residue formed by cleavage of the diethyl groups of the *N,N*-diethylnicotinamide ligand. Molecular ion peaks attributable to acesulfamato, *N,N*-diethylnicotinamide and degradation product nicotinamide molecules in the structure of the complexes were also detected at approximately 161, 177 and 121 m/z regions, respectively. In addition, various peaks that may belong to the leaving products of both acesulfamato and *N,N*-diethylnicotinamide were observed in the mass analysis pattern. Especially peaks belonging to the pyridine ring showed themselves in the 78 m/z area in all complexes. It was also observed in the oxide peaks of the corresponding metal cations, which can be considered as the final cleavage products of the mixed ligand complexes.

3. Conclusion

Complex-ligand complexes of rare earth metal cations (Eu^{3+}, Tb^{3+}, Ho^{3+}, Er^{3+} and Yb^{3+}) containing acesulfamato/*N,N*-diethylnicotinamide were synthesized. Analysis techniques such as elemental analysis, Fourier Transform infrared spectroscopy (FTIR), solid ultraviolet-visible spectroscopy (UV-vis), mass spectroscopy (GC-MS) were studied for the structural properties of the complexes. With the recorded thermal analysis (TGA / DTA) curves, comments were made on the degradation steps of molecules and possible degradation products. According to the chemical composition analysis of the compounds, the metal: ligand1 (*acs*): ligand2 (*dena*) ratios were claimed to be 1:3:2.

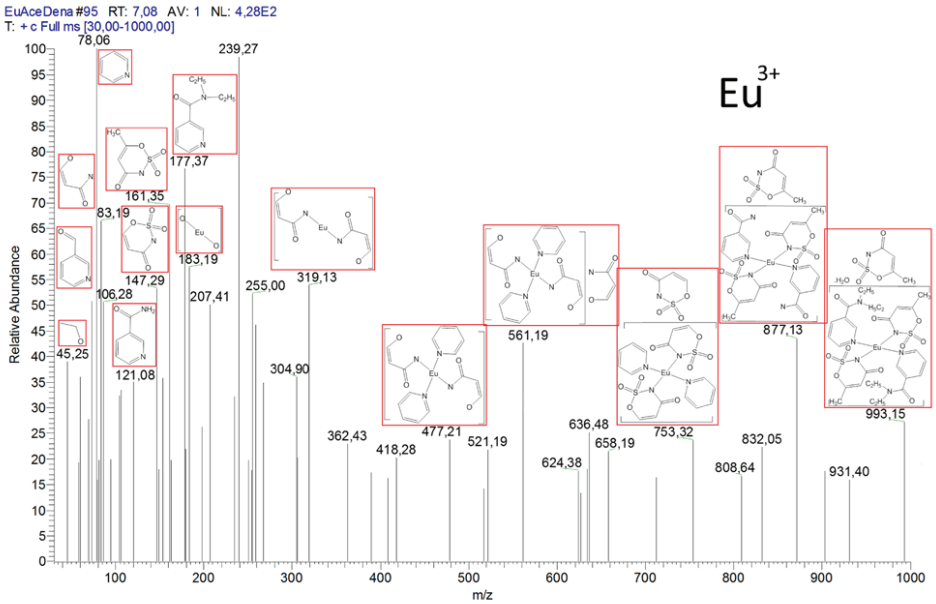

Figure 6. Mass spectra pattern and possible degradation products of mixed ligand complexes of rare-earth metal-acesulfamato/*N,N*-diethylnicotinamide.

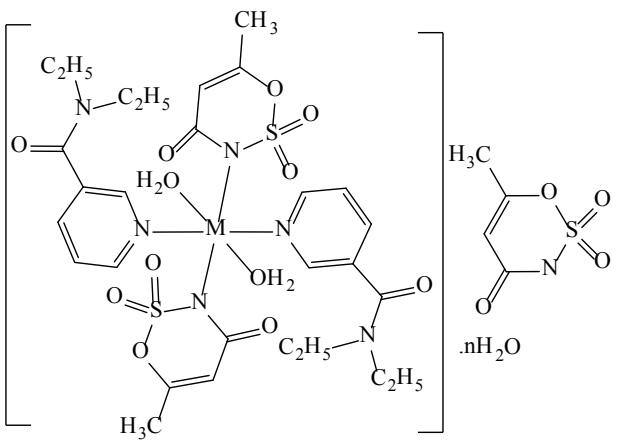

Figure 7. The general structural formula of mixed ligand complexes containing acesulfamato-*N,N*-diethylnicotinamide ligands.

In the structure of complexes, depending on the steric obstacle, two acesulfamato ligands showed monoanionic-monodentate coordination through acidic -N group, while two *N,N*-diethylnicotinamide ligands provided coordination with the metal through the strong electron donor-N- group in the pyridine ring. The M(III) cations, which are predicted to exhibit sixth coordination, complete the coordination circles with two moles of aqua ligands entering the coordination sphere. Metal cations with characteristic 3+ oxidation steps provide their charge balances with an acesulfamato ligand placed as counter ion outside the coordination sphere. Thermal analysis data confirmed that the Ho(III) and Er(III) complexes did not contain any hydrate water except the coordination sphere. Possible temperature-dependent decomposition products of the complexes were also characterized by thermal analysis method, and the compatibility of experimental and theoretical weight loss was confirmed. Since the molecular weight of the complexes is over 1000 g according to the proposed structural formulas.

The molecular ion peaks were not observed in the mass analysis. Besides, according to the results obtained from elemental analysis data, molecular structure formulas proposed for complex structures are supported.

The comparing results obtained from the analysis and measurements with the similar studies in the current literature, it was deemed appropriate to suggest the molecular structure formula in Figure 7 for complex structures containing acesulfamato-*N*,*N*-diethylnicotinamide ligands.

Acknowledgments
The authors acknowledge the Hitit University Unit of Scientific Research Projects (FEF19004.16.004).

References

1. Godlewska P, Hanuza J, Kucharska E, Solarz P, Roszak S et al. Optical and magnetic properties of lanthanide(III) complexes with quercetin-5′-sulfonic acid in the solid state and silica glass. Journal of Molecular Structure 2010; 1219: 128504. doi: 10.1016/j.molstruc.2020.128504
2. Fang M, Shao L-J, Shi T-X, Chen Y-Y, Yu H et al. Four tetra-nuclear lanthanide complexes based on 8-hydroxyquinolin derivatives: magnetic refrigeration and single-molecule magnet behavior. New Journal Chemistry 2018; 42: 11847-11853. doi: 10.1039/C8NJ02161A
3. Gao H-L, Huang S-X, Zhou X-P, Liu Z, Cui J-Z. Magnetic properties and structure of tetranuclear lanthanide complexes based on 8-hydroxylquinoline Schiff base derivative and β-diketone coligand. Dalton Transactions 2018; 47: 3503-3511. doi: 10.1039/C8DT00063H
4. Ning Y, Liu Y-W, Meng Y-S, Zhang J-L. Design of near-infrared luminescent lanthanide complexes sensitive to environmental stimulus through rationally tuning the secondary coordination sphere. Inorganic Chemistry 2018; 57 (3): 1332-1341. doi: 10.1021/acs.inorgchem.7b02750
5. Bouet MC, Eliseeva SV, Aucagne V, Delmas AF, Gillaizeau I, et al. Near-infrared emitting lanthanide(III) complexes as prototypes of optical imaging agents with peptide targeting ability: a methodological approach. RSC Advances 2019; 9: 1747-1751. doi: 10.1039/C8RA09419E
6. GüDen-Silber T, Klein K, Seitz M. 4,4′-Bis (trifluoromethyl)-2, 2′-bipyridine–a multipurpose ligand scaffold for lanthanoid-based luminescence/^{19}F NMR probes. Dalton Transactions 2013; 42: 13882-13888. doi: 10.1039/c3dt50842k
7. Li X, Gu J, Zhou Z, Ma L, Tang Y et al. New lanthanide ternary complex system in electrospun nanofibers: Assembly, physico-chemical property and sensor application. Chemical Engineering Journal 2019; 358: 67-73. doi: 10.1016/j.cej.2018.10.003
8. Kaczmarek MT, Zabiszak M, Nowak M, Jastrzab R. Lanthanides: Schiff base complexes, applications in cancer diagnosis, therapy, and antibacterial activity. Coordination Chemistry Reviews 2018; 370: 42-54. doi: 10.1016/j.ccr.2018.05.012
9. Campello MPC, Palma E, Correia I, Paulo PMR, Matos A et al. Lanthanide complexes with phenanthroline-based ligands: insights into cell death mechanisms obtained by microscopy techniques. Dalton Transactions 2019; 48:4611-4624. doi: 10.1039/C9DT00640K
10. Boroujeni ZA, Bordbar AK, Motlagh MK, Sattarinezhad E, Fani N et al. Synthesis, characterization, and binding assessment with human serum albumin of three bipyridine lanthanide(III) complexes. Journal of Biomolecular Structure and Dynamics 2019; 37 (6): 1438-1450. doi: 10.1080/07391102.2018.1464959
11. Chen H, Cao J, Zhou P, Li X, Xie Y, Liu W, Tang Y, Multiplex recognition and logic devices for molecular robot prototype based on a europium(III)–cyclen system. Biosensors and Bioelectronics 2018; 122: 1-7. doi: 10.1016/j.bios.2018.09.029
12. Wei C, Ma L, Wei HB, Liu ZW, Bian ZQ et al. Advances in luminescent lanthanide complexes and applications. Science China Technological Sciences 2018; 61: 1265-1285. doi: 10.1007/s11431-017-9212-7
13. Bao G. Lanthanide complexes for drug delivery and therapeutics. Journal of Luminescence 2020; 228: 117622. doi: 10.1016/j.jlumin.2020.117622
14. Petrosyants SP. Coordination compounds of rare earth metal thiocyanates. Russian Journal of Coordination Chemistry 2015; 41 (11): 715-729. doi: 10.1134/S107032841511007X
15. Zhang P-F, Yang G-P, Li G-P, Yang F, Liu W-N et al. Series of water-stable lanthanide metal–organic frameworks based on carboxylic acid imidazolium chloride: tunable luminescent emission and sensing. Inorganic Chemistry 2019; 58 (20): 13969-13978. doi: 10.1021/acs.inorgchem.9b01954
16. Du J-Q, Dong J-L, Xie F, Yang R-X, Lan H-M et al. Lanthanide complexes supported via benzimidazole carboxylic acid ligand: Synthesis, luminescence and magnetic properties. Journal of Molecular Structure 2020; 1202: 127345. doi: 10.1016/j.molstruc.2019.127345
17. Liu W, Huang X, Chen C, Xu C, Ma J et al. Function-oriented: the construction of lanthanide MOF luminescent sensors containing dual-function urea hydrogen-bond sites for efficient detection of picric acid. Chemistry A European Journal 2018; 25: 1090-1097. doi: 10.1002/chem.201805080
18. Li Z, Gao F, Xiao Z, Wu X, Zuo J et al. Nonlinear optical properties and excited state dynamics of sandwich-type mixed (phthalocyaninato)(Schiff-base) triple-decker complexes: Effect of rare earth atom. Optics & Laser Technology 2018; 103: 42-47. doi: 10.1016/j.optlastec.2018.01.011

19. Priya J, Sharma SK. Organo lanthanide metal complexes for application as emitting layer in OLEDs. Journal of Materials Science: Materials in Electronics 2018; 29: 180-185. doi: 10.1007/s10854-017-7902-6

20. Zabula AV, Dey S, Robinson JR, Cheisson T, Higgins RF et al. Screening of molecular lanthanide corrosion inhibitors by a high-throughput method. Corrosion Science 2020; 165: 108377. doi: 10.1016/j.corsci.2019.108377

21. Zhang J, Li Y, Hao X, Zhang Q, Yang K et al. Recent progress in therapeutic and diagnostic applications of lanthanides. Mini-Reviews in Medicinal Chemistry 2011; 11 (8): 678-694. doi: 10.2174/138955711796268804

22. Misra SN, Gagnani MA, Devi I, Shukla RS. Biological and clinical aspects of lanthanide coordination compounds. Bioinorganic Chemistry and Applications 2004; 2: 151-192. doi: 10.1155/S1565363304000111

23. Fur ML, Molnár E, Beyler M, Kálmán FK, Fougère O et al. A coordination chemistry approach to fine-tune the physicochemical parameters of lanthanide complexes relevant to medical applications. Chemistry A European Journal 2018; 24 (13): 3127-3131. doi: 10.1002/chem.201705528

24. Huang C, Bian Z. Rare Earth Coordination Chemistry: Fundamentals and Applications. Huang C (editor). Singapore: John Wiley & Sons, 2010, p. 13.

25. Zheng Z. Ligand-controlled self-assembly of polynuclear lanthanide-oxo/hydroxo complexes: from synthetic serendipity to rational supramolecular design. Chemical Communications 2001; 2521-2529. doi: 10.1039/B107971A

26. Bienfait AM, Wolf BM, Törnroos KW, Anwander R. Trivalent rare-earth-metal bis(trimethylsilyl)amide halide complexes by targeted oxidations. Inorganic Chemistry 2018; 57 (9):5204-5212. doi: 10.1021/acs.inorgchem.8b00240

27. Schumann H, Freckmann DMM, Dechert S. Organometallic compounds of the lanthanides. 183 lanthanide benzyl complexes of the type $[Li(tmeda)_2][Ln(CHRSiMe_2R')_3Cl]$ (Ln = Pr, Nd, Sm, Er, Lu; R = Ph, 3,5-$Me_2C_6H_3$; R′=Me, tBu, Ph) and $[Li(tmeda)]2(\mu\text{-}Cl)_3Ln(CHPhSiMe_2tBu)_2$ (Ln = Er, Lu Zeitschrift für anorganische und allgemeine Chemie 2008; 634: 2199-2208. doi: 10.1002/zaac.200800167

28. Petrosyants SP. Coordination polymers of indium, scandium, and yttrium. Russian Journal of Inorganic Chemistry 2013; 58 (13): 1605-1624. doi: 10.1134/S0036023613130032

29. Kremera C, Torresa J, Dominguez S, Mederos A. Structure and thermodynamic stability of lanthanide complexes with amino acids and peptides. Coordination Chemistry Reviews 2005; 249 (5-6): 567-590. doi: 10.1016/j.ccr.2004.07.004

30. Clauss K, Jensen H. Oxatiazinon dioxides a new group of sweetening agents. Angewandte Chemie International Edition in English 1973; 12: 869-876. doi: 10.1002/anie.197308691

31. Mukherjee A, Chakrabarti J. In vivo exposed to cytogenetic studies on mice acesulfame-K a non-nutritive sweetener. Food and Chemical Toxicology 1997; 35 (12): 1177-1179. doi: 10.1016/S0278-6915(97)85469-5

32. Duffy VB, Anderson GH. Use of nutritive and non-nutritive sweetener. Journal of the American Dietetic Association 1998; 98: 580-587. doi: 10.1016/s0002-8223(98)00131-x

33. Yurdakul O, Kose DA. Mixed ligand complexes of acesulfame/nicotinamide with earth alkaline metal cations MgII, CaII, BaII and SrII. Synthesis and characterization. Hitite Journal of Science and Engineering 2014; 1 (1): 51-57. doi: 10.17350/HJSE19030000008

34. Yıldırım T, Köse DA, Avcı E, Özer D, Şahin O. Novel mixed ligand complexes of acesulfame / nicotinamide with some transition metals. Synthesis, crystal structural characterization, and biological properties. Journal Molecular Structure 2019; 1176: 576-582. doi: 10.1016/j.molstruc.2018.08.099

35. Yıldırım T, Köse DA, Avcı GA, Şahin O, Akkurt F. Novel mixed ligand complexes of acesulfame/*N,N*-diethylnicotinamide with some transition metals. Synthesis and crystal structural characterization. Journal of Coordination Chemistry 2019; 72 (22-24): 3502-3517. doi: 10.1080/00958972.2019.1705970

36. Yurdakul Ö, Köse DA, Şahin O, Avcı GA. Two novel mixed-ligand zinc-acesulfame compounds: Synthesis, spectroscopic and thermal characterization and biological applications. Journal Molecular Structure 2020; 1203: 127265. doi: 10.1016/j.molstruc.2019.127265

37. Icbudak H, Uyanik A, Bulut A, Arıcı C, Ulku D. Synthesis, thermal, spectroscopic and structural properties of di(aqua)bis(N,N¢-dimethylethylenediamine-k^2N,N¢)copper(II) acesulfamate. Zeitschrift für Kristallographie 2007; 222 (8): 432-436. doi: 10.1524/zkri.2007.222.8.432

38. Bulut A, Icbudak H, Sezer G, Kazak C. Bis(acesulfamatok^2N^3,O^4)bis(2-aminopyrimidine-kN^1)copper(II). Acta Crystallographica 2005; C61: m228-m230. doi: 10.1107/S0108270105008188

39. Icbudak H, Bulut A, Cetin N, Kazak C. Bis(acesulfamato)- tetraaquacobalt(II). Acta Crystallographica 2005; C61: m1-m3. doi: 10.1107/S0108270104028574

40. Icbudak H, Adiyaman E, Cetin N, Bulut A, Buyukgungor O. Synthesis, structural characterization and chromotropism of a Ni(II) and a Co(II) compound with acesulfamate as a ligand. Transition Metal Chemistry 2006; 31: 666-672. doi: 10.1007/s11243-006-0045-x

41. Topçu Y, Andaç Ö, Yılmaz VT, Harrison WTA. Synthesis, characterization and spectral studies of triethanolamine complexes of metal saccahrinates. Crystal structures of $[Co(tea)_2](sac)_2$ and $[Cu_2(m\text{-}tea)_2(sac)_2].2(CH_3OH)$. Journal of Coordination Chemistry 2002; 55: 805-815. doi: 10.1080/0095897022000001557

42. Yılmaz VT, Topcu Y, Yılmaz F, Thoene C. Saccharin complexes of Co(II), Ni(II), Cu(II), Zn(II), Cd(II) and Hg(II) with ethanolamine and diethanolamine: synthesis, spectroscopic and thermal characteristics. Crystal structures of $[Zn(ea)_2(sac)_2]$ and $[Cu_2(m\text{-}dea)_2(sac)_2]$. Polyhedron 2001; 20: 3209-3217. doi: 10.1016/S0277-5387(01)00930-5

43. Yılmaz VT, Güney S, Andaç Ö, Harrison WTA. Differernt coordination modes of saccharin in the metal complexes with 2- pyridiylmethanol: synthesis, spectroscopic, thermal and structural characterization. Polyhedron 2002; 21: 2393-2402. doi: 10.1016/S0277-5387(02)01211-1